Ga-doped ZnO films grown on GaN templates by plasma-assisted molecular-beam epitaxy

H. J. Ko, Y. F. Chen, S. K. Hong, H. Wenisch, T. Yao, and D. C. Look

---

Articles you may be interested in

Effects of gallium doping on properties of a -plane ZnO films on r -plane sapphire substrates by plasma-assisted molecular beam epitaxy
J. Vac. Sci. Technol. A **29**, 03A111 (2011); 10.1116/1.3562162

Ga-related photoluminescence lines in Ga-doped ZnO grown by plasma-assisted molecular-beam epitaxy
Appl. Phys. Lett. **94**, 072101 (2009); 10.1063/1.3080204

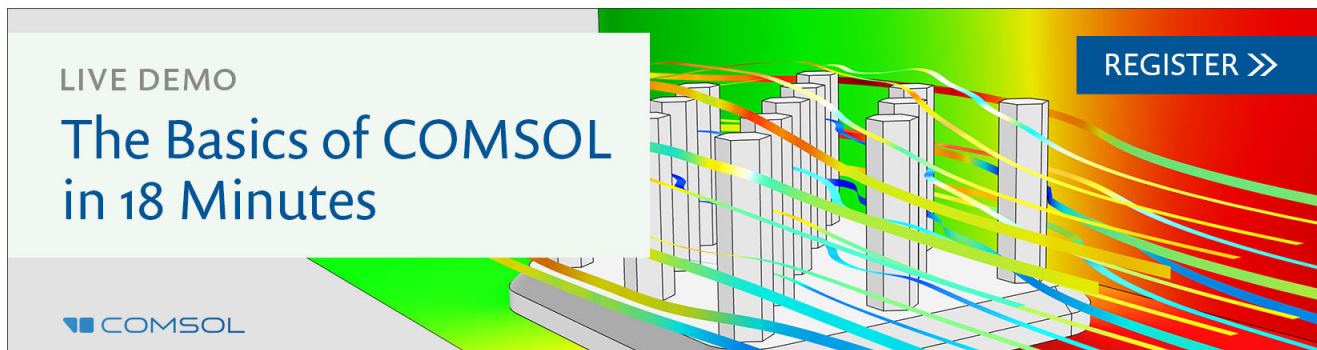Photoluminescence of Ga-doped ZnO film grown on c - Al 2 O 3 (0001) by plasma-assisted molecular beam epitaxy
J. Appl. Phys. **102**, 073114 (2007); 10.1063/1.2783956

Control of polarity of ZnO films grown by plasma-assisted molecular-beam epitaxy: Zn- and O-polar ZnO films on Ga-polar GaN templates
Appl. Phys. Lett. **77**, 3571 (2000); 10.1063/1.1329865

Structural and optical properties of lattice-matched ZnBeSe layers grown by molecular-beam epitaxy onto GaAs substrates
Appl. Phys. Lett. **70**, 3564 (1997); 10.1063/1.119234

Ga-doped ZnO films grown on GaN templates by plasma-assisted molecular-beam epitaxy

H. J. Ko,[a)] Y. F. Chen, S. K. Hong, H. Wenisch, and T. Yao
Institute for Materials Research, Tohoku University, Katahira, Aoba-Ku, Sendai 980-8577, Japan

D. C. Look
Semiconductor Research Center, Wright State University, Dayton, Ohio 45435

We have investigated the structural and optical properties of Ga-doped ZnO films grown on GaN templates by plasma-assisted molecular-beam epitaxy. The carrier concentration in Ga-doped ZnO films can be controlled from 1.33×10^{18}/cm^3 to 1.13×10^{20}/cm^3. Despite high Ga incorporation, the linewidth of (0002) ω-rocking curves of Ga-doped ZnO films still lies in the range from 5 to 15 arc min. Photoluminescence (PL) spectra of Ga-doped ZnO films show dominant near-bandedge emission with negligibly weak deep-level emission, independent of carrier concentration. The PL spectrum exhibits a new emission line at 3.358 eV, which corresponds to exciton emission bound to a Ga donor. To avoid degradation of the PL intensity, the maximum dopability of Ga in ZnO is determined to be around 2.6×10^{19}/cm^3.   © *2000 American Institute of Physics.*
[S0003-6951(00)02050-7]

ZnO is a II–VI compound semiconductor with a direct band gap of 3.37 eV at room temperature. Recently, it has attracted considerable attention because of its large exciton binding energy of 60 meV. This large exciton binding energy enables optically pumped excitonic lasing at room temperature,[1,2] and high-temperature stimulated emission up to 550 K due to exciton mechanism.[3] So far, high-quality ZnO layers have been grown either pulsed laser deposition[4] or plasma-assisted molecular-beam epitaxy (P–MBE).[5,6] ZnO layers can be grown in a layer-by-layer mode,[5,6] which have lead to the growth of ZnO layers with high quality enough to show biexciton emission.[7] The next major focus will be on conductivity control by impurity doping.

Undoped ZnO films generally exhibit n-type conduction with typical carrier concentration of $\sim 10^{17}$/cm^3.[8,9] It should be mentioned that the control of carrier concentration in n-type ZnO has not been achieved yet for single-crystalline epilayers, although carrier concentration in a range from 10^{18} to 10^{20}/cm^3 will be needed for laser-diode application. This letter will report on the control of carrier concentration of n-type ZnO films up to $\sim 10^{20}$/cm^3 by doping with Ga.

Group III elements Al, Ga, In, and group VII elements Cl and I can be used as n-type dopants in P–MBE of ZnO films. Because of high reactivity of Al, oxidation of the Al source during ZnO growth may become a problem. Ga and In are less reactive and more resistive to oxidation, compared to Al. Cl and I may have a memory effect, so that the residual electron concentration would not be low after Cl or I were used. On the other hand, the covalent bond lengths of Ga–O and Zn–O are estimated to be 1.92 and 1.97 Å, respectively using atomic radii,[10] which should be compared with those of In–O (2.1 Å) and Zn–Cl (2.3 Å). A slightly smaller bond length of Ga–O than that of Zn–O is expected

to make the deformation of the ZnO lattice small even in the case of high Ga concentration, while the larger bond lengths of In–O and Zn–Cl would deform the ZnO lattice more seriously. This is why Ga has been selected as a n-type dopant in ZnO in our experiments.

Ga-doped ZnO films have been grown on 4-μm-thick epitaxial GaN layers by P–MBE. The epitaxial GaN was n type with a carrier concentration of 6×10^{16}/cm^3. The growth of Ga-doped ZnO films was carried out at 750 °C with a Zn equivalent flux of 1.5 Å/s and an oxygen flow rate of 1.5 sccm, which gave rise to an oxygen rich condition. The thickness of the Ga-doped ZnO films was around 0.65 μm.

Figure 1 shows room temperature carrier concentrations (dots) of Ga-doped ZnO films measured by the van der Pauw method as a function of Ga cell temperature, and the calcu-
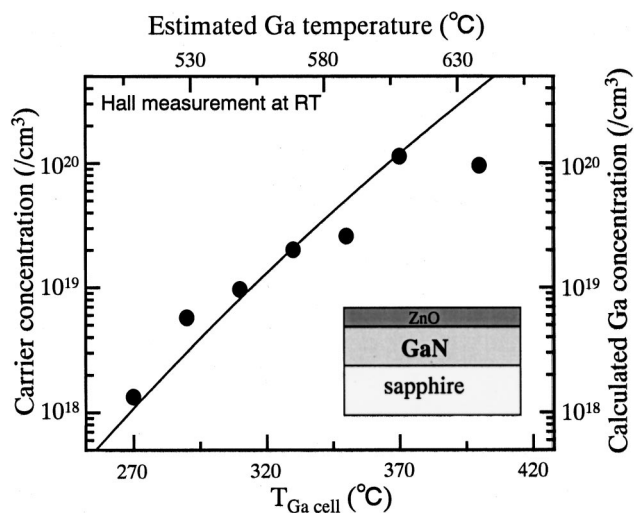

FIG. 1. Carrier concentration (dots) of n-type ZnO films doped with Ga as a function of Ga cell temperature and calculated Ga concentration (solid line) vs estimated Ga temperature.

[a)]Author to whom correspondence should be addressed; electronic mail: koko@imr.tohoku.ac.jp
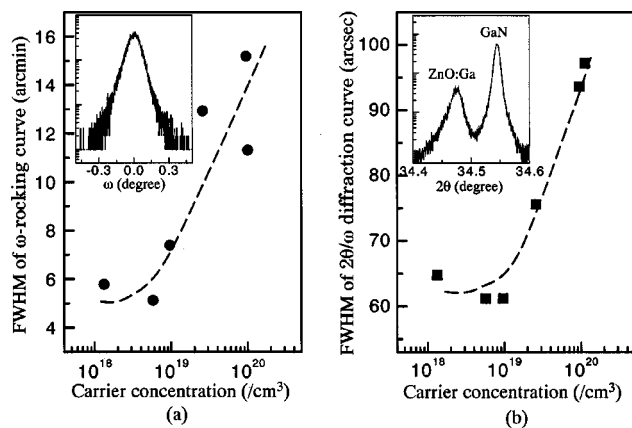
FIG. 2. FWHM values of (a) ω-rocking curve and (b) $2\theta/\omega$ diffraction curve of the (0002) reflection of Ga-doped ZnO films as a function of carrier concentration. Insets show (a) ω-rocking curve and (b) $2\theta/\omega$ diffraction curve of the (0002) reflection of a Ga-doped ZnO film with a carrier concentration of $9.6 \times 10^{18}/cm^3$.

FIG. 3. (a) PL spectrum for Ga-doped ZnO film with a carrier concentration of $5.7 \times 10^{18}/cm^3$, and (b) bound exciton emission spectra of undoped ZnO (dotted curve) and Ga-doped ZnO (solid curve) films.

lated Ga concentration (solid curve) versus estimated Ga source temperature. The Ga concentration (N_{Ga}) incorporated in the films was calculated by $N_{Ga} = p[N_A/(2\pi m_{Ga}k_B T_{Ga})]^{1/2}/v_G$, where p is the vapor pressure of Ga, N_A and k_B are the Avogadro and Boltzmann constants, respectively, m_{Ga} and T_{Ga} are the Ga atom weight and the estimated Ga source temperature, respectively, and v_G is the growth rate. As the Ga cell temperature increases from 270 to 400 °C, the electron concentration increases exponentially from $1.33 \times 10^{18}/cm^3$ to $1.13 \times 10^{20}/cm^3$, and the electron mobility (μ) decreases ($\mu = 120.5$ cm^2 V^{-1} s^{-1} for $1.33 \times 10^{18}/cm^3$, $\mu = 36.7$ cm^2 V^{-1} s^{-1} for $2.58 \times 10^{19}/cm^3$, and $\mu = 51.1$ cm^2 V^{-1} s^{-1} for $9.53 \times 10^{19}/cm^3$). The increment of carrier concentration up to around $10^{20}/cm^3$ is in good agreement with the variation of calculated Ga concentration, which suggests that most of the incorporated Ga atoms form shallow donors and are activated at room temperature. As the Ga cell temperature exceeds 400 °C, the carrier concentration shows a tendency toward saturation due to an onset of carrier compensation.

Figure 2 shows full width at half maximum (FWHM) values of (a) ω-rocking curves and (b) $2\theta/\omega$ diffraction curves of the (0002) reflection of Ga-doped ZnO films as a function of carrier concentration. The insets in Fig. 2 show typical diffraction curves of the (0002) reflection of a ZnO film with a carrier concentration of $9.6 \times 10^{18}/cm^3$ for both ω and $2\theta/\omega$ scans. The line profiles for both diffraction curves are well fitted by Gaussian curves, which implies that Ga doping causes neither degradation of interface nor serious change in crystal structure, even at high doping level up to $\sim 10^{20}/cm^3$. As the carrier concentration in Ga-doped ZnO layers increases from $1.33 \times 10^{18}/cm^3$ to $1.13 \times 10^{20}/cm^3$, both FWHM values for ω and $2\theta/\omega$ diffraction curves gradually increase from 5 to 15 arc min and 61 to 94 arc sec, respectively. Such a gradual increase in the linewidth of diffraction curves is generally observed in impurity doped crystals and can be attributed to increase in local strain around impurity atoms or point defects associated with the impurity atoms.[11,12] We note, however, such a gradual increase in FWHM value would be overtaken by an abrupt increase when a considerable change in lattice structure occurred,
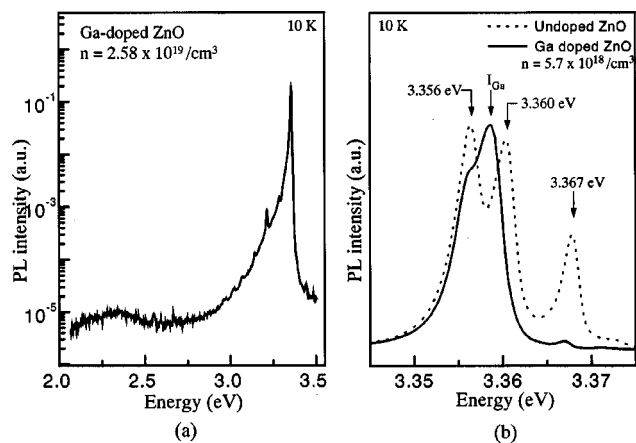
such as formation of small angle grain boundaries, generation of dislocations, and stacking faults. It should also be noted that the FWHM values of the (0002) ω-rocking curves of Ga-doped ZnO layers lie in the range of undoped ZnO layers.[13] We stress that despite high Ga doping, ZnO films exhibit only slight degradation in crystal structure.

Figure 3(a) shows a low temperature photoluminescence (PL) spectrum of a Ga-doped ZnO layer with a carrier concentration of $2.58 \times 10^{19}/cm^3$. The excitation intensity of the 325 nm line from a He–Cd laser was 80 mW/cm^2. The bound excitonic emission dominates the PL spectrum [Fig. 3(a)], while deep-level emission at around 2.3 eV is negligibly weak. The deep-level emission intensity shows only slight variation with carrier concentration as shown in Fig. 4, although the x-ray diffraction linewidth increases with carrier concentration (Fig. 2). These facts imply that Ga doping does not contribute to the creation of defects responsible for the deep-level emission, but it produces local strain around Ga atoms or point defects associated with Ga impurities which do not affect the deep-level emission.

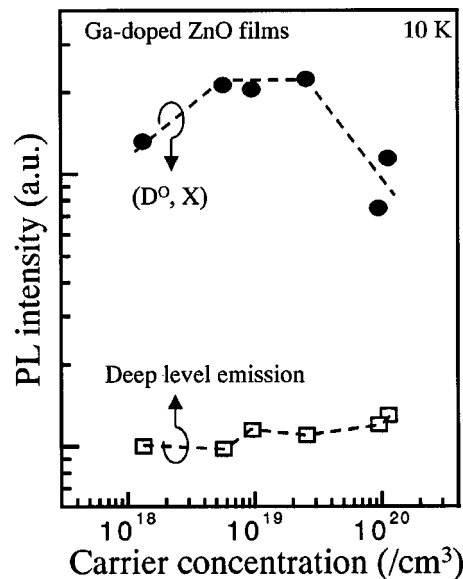Figure 3(b) shows details of the bound exciton emission

FIG. 4. Integrated PL intensity of I_{Ga} emission for Ga-doped ZnO films as a function of carrier concentration.

spectra of undoped ZnO (dotted curve) and Ga-doped ZnO (solid curve) films with a carrier concentration of 5.7×10^{18}/cm^3. The bound exciton emission lines at 3.356, 3.360, and 3.367 eV dominate the PL spectrum of undoped ZnO films. These emission lines could be correlated with defect complexes, as was conjectured in an earlier work.[14] In that case, after a high-temperature anneal, only the lowest-energy (3.356 eV) exciton survived. It is noted that Ga doping makes a considerable change in the bound exciton emission spectrum. The PL spectrum of Ga-doped ZnO shows a new emission line at 3.358 eV which hereafter is called I_{Ga}. The emission line at 3.360 eV disappears, while emission lines at 3.356 and 3.367 eV are greatly reduced in intensity. We suggest that the newly observed emission line I_{Ga} can be ascribed to bound exciton emission associated with a Ga donor.

The integrated PL intensity of I_{Ga} emission is plotted in Fig. 4 as a function of carrier concentration at room temperature. The PL intensity increases with increasing carrier concentration up to 5.7×10^{18}/cm^3. Then, it shows a saturation behavior until 2.58×10^{19}/cm^3, beyond which it decreases abruptly. The same such behavior is generally observed in impurity-doped semiconductors and is understood in the following manner: The increase of the PL intensity in the low carrier concentration regime is due to an increase in the intensity of the impurity-related emission, which is the Ga-donor related exciton emission I_{Ga} in the present case. However, the doping of impurities higher than a certain threshold would generate defects. Those defects would reduce the emission intensity by introducing either radiative deep levels or nonradiative channels. At high doping levels impurity clusters or impurity-defect complexes may limit radiative efficiency.[15] A similar phenomenon was observed by Tsang *et al.*[16] in GaP crystals. They interpreted the behavior of their bound exciton emission as being due to nonradiative Auger recombination processes associated with delocalized electrons in the impurity band. It is suggested from Fig. 4 that those two competing factors balance in the carrier concentration range of 10^{19}/cm^3 and the formation of defects or nonradiative channels dominates for carrier concentration higher than 3×10^{19}/cm^3, presumably due to the onset of carrier compensation as is observed in Fig. 1. We conclude that the dopability of Ga in ZnO is limited to 2.6×10^{19}/cm^3, at least in terms of PL.

In conclusion, we have demonstrated that the carrier concentration in *n*-type ZnO films grown by P–MBE on GaN templates can be well controlled from 1.33×10^{18}/cm^3 to 1.13×10^{20}/cm^3. The effective doping of Ga, with minimized carrier compensation, is achieved even for the high carrier concentration of 1.13×10^{20}/cm^3. The FWHM value of the (0002) x-ray rocking curves of the Ga-doped ZnO films increases from 5 to 15 arc min with increasing carrier concentration, which is still within the FWHM values of undoped ZnO films. Low-temperature PL spectra of Ga-doped ZnO show dominant bound exciton emission at 3.358 eV and negligibly weak deep-level emission at around 2.3 eV. This bound exciton emission emerges by Ga doping and overtakes the bound exciton emissions observed in undoped ZnO layers. The intensity of I_{Ga} emission increases with carrier concentration up to 5.7×10^{18}/cm^3, shows a saturation behavior from 5.7×10^{18}/cm^3 to 2.58×10^{19}/cm^3, and eventually rapidly decreases above 2.58×10^{19}/cm^3. The maximum dopability of Ga in ZnO is inferred to be around 2.6×10^{19}/cm^3, if PL quality is used as a criterion.

[1] D. M. Bagnall, Y. F. Chen, Z. Zhu, T. Yao, S. Koyama, M. Y. Shen, and T. Goto, Appl. Phys. Lett. **70**, 2230 (1997).
[2] Z. K. Tang, G. K. L. Wong, P. Yu, M. Kawasaki, A. Ohtomo, H. Koinuma, and Y. Segawa, Appl. Phys. Lett. **72**, 3270 (1998).
[3] D. M. Bagnall, Y. F. Chen, Z. Zhu, T. Yao, M. Y. Shen, and T. Goto, Appl. Phys. Lett. **73**, 1038 (1998).
[4] R. D. Vispute, V. Talyansky, S. Choopun, R. P. Sharma, T. Venkatesan, M. He, X. Tang, J. B. Halpern, M. G. Spencer, Y. X. Li, L. G. Salamanca-Riba, A. A. Iliadis, and K. A. Jones, Appl. Phys. Lett. **73**, 348 (1998).
[5] H. J. Ko, Y. F. Chen, S. K. Hong, and T. Yao, J. Cryst. Growth **209**, 816 (2000).
[6] Y. F. Chen, H. J. Ko, S. K. Hong, and T. Yao, Appl. Phys. Lett. **76**, 559 (2000).
[7] H. J. Ko, Y. F. Chen, and T. Yao, Appl. Phys. Lett. **77**, 537 (2000).
[8] S. Bethke, H. Pan, and B. W. Wessels, Appl. Phys. Lett. **52**, 138 (1988).
[9] S. Choopun, R. D. Vispute, W. Noch, A. Balsamo, R. P. Sharma, T. Venkatesan, A. Iliadis, and D. C. Look, Appl. Phys. Lett. **75**, 3947 (1999).
[10] C. Kittel, *Introduction to Solid State Physics*, 6th ed. (Wiley, New York, 1986), p. 76.
[11] T. Nina, T. Minato, and K. Yoneda, Jpn. J. Appl. Phys., Part 2 **21**, L387 (1982).
[12] K. Ohkawa, T. Mitsuyu, and O. Yamazaki, J. Appl. Phys. **62**, 3216 (1987).
[13] H. J. Ko, Y. F. Chen, S. K. Hong, H. Wenisch, and T. Yao (private communication).
[14] D. C. Reynolds, D. C. Look, B. Jogai, C. W. Litton, T. C. Collins, W. Harsch, and G. Cantwell, Phys. Rev. B **57**, 12151 (1998).
[15] V. Swaminathan and A. T. Macrander, *Materials Aspects of GaAs and InP Based Structures* (Prentice-Hall, Englewood Cliffs, NJ, 1991), p. 319.
[16] J. C. Tsang, P. J. Dean, and P. T. Landsberg, Phys. Rev. **173**, 814 (1968).